Pergamon

Int. J. Heat Mass Transfer. Vol. 39, No. 2, pp. 331–346, 1996
Elsevier Science Ltd.
Printed in Great Britain

0017-9310(95)00121-2

The second moments, spectra and correlation functions of velocity and temperature fluctuations in the gradient sublayer of a retarded boundary layer

B. A. KADER
35 Orkney Road, No.5, Brookline, MA 02146, U.S.A.

(*Received* 30 *March* 1994 *and in final form* 10 *March* 1995)

Abstract—The turbulent structure of velocity and temperature fields in moving equilibrium retarded boundary layers is analyzed. Most attention is given to 'the gradient sublayer', where, according to Ginevskii and Solodkin [*Prikl. Mat. Mech.* (*Appl. Math. Mech.*) **22**, 819–825 (1958)], Stratford [*J. Fluid Mech.* **5**, 1–16; 17–35 (1959)] and Perry *et al.* [*J. Fluid Mech.* **25**, 299–320 (1966)], the mean velocity and temperature profiles are described by the half-power and inverse half-power laws. Kader [*Dokl. Akad. Nauk U.S.S.R.* **279**, 323–327 (1984); *Int. J. Heat Mass Trans.* **34**, 2837–2857 (1991)] deduced formulas for spectra and cospectra of velocity components and temperature in the gradient sublayer for the mesoscale range of wave numbers k by dimensional analysis and then compared them with available experimental data. It is shown that accurate determination of velocity variances and Reynolds stresses requires taking into account the contribution of large-scale turbulent disturbances corresponding to small values of k. It is not so for determination of the temperature variance and vertical heat flux evaluation. An analysis of low wave number parts of velocity and temperature spectra and cospectra is given, and its results are used to determine the correlation functions of turbulent fluctuations in the gradient sublayer. The formulas for one-point second-order moments (variances $\langle t^2\rangle$, $\langle u^2\rangle$ and $\langle v^2\rangle$, temperature flux $\langle vt\rangle$, and Reynolds stress $\langle -uv\rangle$) in the gradient sublayer of quasi-equilibrium flows are also derived and compared with the available data. Comparison of calculated and experimental spectra of non-equilibrium retarded flows uncovers disagreement in the mesoscale wave number part of the spectra for vertical velocity and Reynolds stress fluctuations. At the same time longitudinal fluctuation spectra and one-point variance $\langle u^2\rangle$ prove to be less sensitive to non-equilibrium conditions.

1. INTRODUCTION

Pressure-gradient boundary layers are of great importance for engineering and thermo-fluid mechanics. Aside from the many important practical applications of the gradient boundary layers, any information that leads to a better understanding of the effect of longitudinal pressure gradient on the turbulent structure will be a significant scientific contribution. Therefore, it is not surprising that there is an enormous amount of literature devoted to the study of gradient turbulent flows, but most of it concerns only mean velocity profiles U. According to experiments (see, e.g. refs. [1–3]), dimensional arguments [1, 2, 4, 5], calculations based on simple semiempirical models related to Prandtl's mixing length theory (e.g. refs. [1, 3, 6]) or more sophisticated closure models (e.g. refs. [7, 8]), there are three distinguished zones in retarded moving-equilibrium boundary layers not near to separation: the outer part, where mean velocity U and temperature T profiles are described by defect laws; the inner part, where ordinary wall laws are valid; and the intermediate sublayer, where U and T profiles are determined by special 'gradient laws'. Alas, the conclusions made on the basis of this scheme are often very controversial, so a number of authors using the asymptotic expansion method (see, e.g. ref. [9]) came to the conclusion that a velocity profile in the intermediate sublayer can be described by a logarithmic law with coefficients depending on mean pressure gradient, while in other papers (e.g. in ref. [8]), based again on the asymptotic expansion method, it was found that there is no logarithmic sublayer at all. This conclusion was supported by experiments in pressure-gradient boundary layers near to separation [1, 2].

There are many more examples of such contradictions but at least some of them can be explained by simple dimensional considerations. This was done, for example, in refs. [5, 10], where the three-layer model was proposed for a moving-equilibrium boundary layer with a mild value of adverse pressure gradient.

The model of retarded boundary layer under consideration is based on the assumption that the turbulent structure of the analyzed flow depends on the following dimensional parameters: molecular viscosity and diffusivity ν and χ, friction velocity u_*, temperature flux $Q = \langle vt\rangle$, kinematic pressure gradient $\gamma = \rho^{-1}\,\mathrm{d}P/\mathrm{d}x$, and thicknesses of dynamic and temperature boundary layers δ and H. Instead of them, the following five length scales can be used: the

NOMENCLATURE

E_u, E_v, E_w, E_t longitudinal spectra of u, v, w and t fluctuations
E_{uv}, E_{vt}, E_{ut} longitudinal cospectra of Reynolds stresses $\langle -uv \rangle$, vertical $\langle vt \rangle$ and horizontal $\langle ut \rangle$ heat fluxes
H thickness of a thermal boundary layer
k wave number
l_K, l_t, v_K, t_K viscous and diffusive length, velocity, and temperature Kolmogorov microscales, $(\nu^3/\varepsilon)^{1/4}$, $(\chi^3/\varepsilon)^{1/4}$, $(\nu\varepsilon)^{1/4}$, $(N^2\nu/\varepsilon)^{1/4}$, respectively
N rate of dissipation for $\langle t^2/2 \rangle$
Pe_* Peclet number, $\delta/\delta_h = \delta u_*/\chi$
Pr thermal or diffusion Prandtl number, ν/χ
dP/dx longitudinal pressure gradient
Q temperature flux, $\langle vt \rangle$
Re_* friction velocity Reynolds number, $\delta/\delta_v = \delta u_*/\nu$
S $\delta_p/\delta_v = u_*^3/\gamma\nu$
t temperature fluctuations
t_* temperature scale, Q/u_*
T mean temperature
U mean longitudinal velocity
U_∞ free-stream velocity
u_* friction velocity
u, v, w velocity fluctuations along the x-, y-, z-axes, respectively
x, y, z longitudinal, vertical and transverse coordinates, respectively
Y $y/\delta_p = \gamma y/u_*^2$
Z $\delta/\delta_p = \gamma\delta/u_*^2$
$\langle\ \rangle$ averaging symbol.

Greek symbols
γ kinematic pressure gradient, $\rho^{-1}\,dP/dx$
δ thickness of a dynamic boundary layer
δ_v, δ_h, δ_p viscosity, diffusivity and pressure gradient length scales, respectively, ν/u_*, χ/u_*, u_*^2/γ
ε mean energy dissipation rate
ν molecular viscosity
ρ density
χ molecular diffusivity.

Subscripts
p quantities made dimensionless by pressure gradient parameters γ, δ, Q
$+$ quantities made dimensionless by wall parameters ν, χ, u_* and Q.

viscous and diffusive length scales ν/u_* and χ/u_*; the pressure gradient length scale $\delta_p = u_*^2/\gamma$; and outer flow length scales δ and H, which, for the sake of simplicity, we will assume have close values. If these length scales satisfy the inequalities

$$\max(\delta_v, \delta_h) \ll \delta_p \ll \min(\delta, H)$$

then the turbulent boundary layer is a fully developed one (Reynolds and Peclet numbers $Re_* = \delta u_*/\nu = \delta/\delta_v$ and $Pe_* = \delta u_*/\chi = \delta/\delta_h$ are high enough) and according to refs. [4, 5] three special zones can be singled out (see Fig. 1), as given below.

If $y \ll \delta_p = u_*^2/\gamma$, then it is natural to assume that neither δ_p (and therefore γ) nor δ and H affect the turbulence regime significantly. Therefore, the mean characteristics of turbulence [including mean velocity and temperature profiles $U(y)$ and $T(y)$] depend only on ν, χ, u_*, Q and y. Hence, at $y \ll \delta_p$ we have the wall layer, where ordinary velocity and temperature laws of constant-pressure boundary layers (presented, for example, in ref. [11]) are valid.

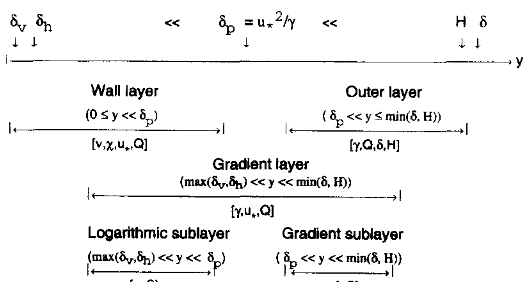

Fig. 1. The validity ranges for similarity laws in a retarded turbulent boundary layer. The main dimensional parameters determining the turbulent structure in the given range of y values are indicated in square brackets.

If $\max(\delta_v, \delta_h) \ll y \ll \min(\delta, H)$ (see Fig. 1) the parameters ν, χ, δ and H are not important and the turbulent structure depends only on γ, u_* and Q.

For a layer far from the wall, where $y \gg \delta_p$ (and hence *a fortiori* $y \gg \delta_v$, δ_h) the defect laws must be valid. However, according to refs. [4, 5], contrary to constant-pressure flows [11], the velocity and temperature scales are different from simple friction scales u_* and $t_* = Q/u_*$ but are given as $u_{**} = (\gamma\delta)^{1/2}$ and $t_{**} = Q/(\gamma H)^{1/2}$.

Moreover, if there is an overlapping region $\max(\delta_v, \delta_h) \ll y \ll \delta_p$ (see Fig. 1), where both wall-layer laws (valid in the region $0 \leqslant y \ll \delta_p$) and gradient laws [in the region $\max(\delta_v, \delta_h) \ll y \ll \min(\delta, H)$] are simultaneously valid, then in this region all the similarity laws must have the same form as in the logarithmic sublayer of a constant-pressure boundary layer [11], i.e. here

$$U_+(y) = A \ln y_+ + B \quad T_+(y) = \alpha \ln y_+ + \beta(Pr) \tag{1}$$

where $y_+ = y/\delta_v = yu_*/\nu$, $U_+ = U/u_*$, $T_+ = [T(0) -$

$T(y)]/t_*$, A, B and α are universal constants, and $\beta(Pr)$ is a universal function of the Prandtl number $Pr = \nu/\chi$.

In the overlapping region $\delta_p \ll y \ll \delta$, if this zone exists, there are 'gradient laws'

$$U_+(y) = KY^{1/2} + K_1(S)$$
$$T_+(y) = -\lambda Y^{-1/2} + \lambda_1(S, Pr) \qquad (2)$$

(see, e.g. [2, 5]). Here $Y = y/\delta_p = y\gamma/u_*^2$, $S = \delta_p/\delta_v = u_*^3/\gamma\nu$, K and λ are universal constants, and $K_1(S)$, $\lambda_1(S, Pr)$ are universal functions, which are determined by the difference of mean velocity and temperature between a wall and lower boundary of 'gradient sublayer', where the mean velocity and temperature profiles are described by the 'half-power law' and 'inverse power law' (2).

All these mean profile laws (1) and (2) were carefully compared with available experiments in refs. [1, 2, 4, 5], where also the cases of small and large pressure-gradient flows were studied. According to the scheme in Fig. 1 the kinematic pressure gradient must be considered as a small one if $\delta_p > \delta$, i.e. $Z = \delta/\delta_p = \gamma\delta/u_*^2 < 1$. Therefore, the gradient sublayer does not exist in such a flow but if $\delta \gg \max(\delta_v, \delta_h)$ then there is a noticeable logarithmic sublayer.

In the other asymptotic case of large pressure gradient, where δ_p is of the order of $\max(\delta_v, \delta_h)$, the logarithmic sublayer vanishes and the gradient sublayer (2) is found between the wall and outer region. In fact, it is just enough to have $\delta_p < (30\text{–}60)\delta_v$ (the lower boundary of logarithmic sublayer) to exclude the logarithmic zone (1). This is the reason why in a pressure-gradient boundary layer near separation the logarithmic sublayer does not exist (see, e.g. refs. [1, 2, 8]).

For pressure-gradient turbulent boundary layers the gradient sublayer plays the same role as the log-sublayer in constant-pressure wall flows. In particular, the formulas (2) lead to the friction law [5] and the heat-mass-transfer law [4] in pressure gradient flows.

There are enough experimental data in the literature to evaluate the unknown coefficients and functions included in these equations. At the same time the study of the turbulent structure of the gradient sublayer has attracted relatively little attention though it is known that the longitudinal adverse pressure gradient strongly affects the turbulent fluctuations here. This is mainly explained by the great experimental difficulties of such studies and the lack of theoretical work devoted to the turbulence structure of pressure gradient flows. This shortage especially concerns the measurements of spectra for velocity and temperature fluctuations in the gradient sublayer. The most comprehensive measurements were implemented in refs. [3, 12–14]. In refs. [12, 13] only velocity fluctuations in the conical diffuser were measured. Roganov's study [3] contains the most complete set of experimental data measured in the adverse gradient boundary layer on a heated plate, and this study is of special interest for the present paper.

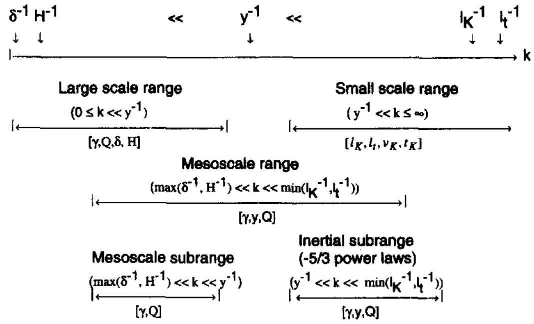

Fig. 2. The validity ranges for spectral similarity laws in the retarded turbulent boundary layer. The main dimensional parameters determining the spectral shapes in the given range of k values are indicated in square brackets.

2. VELOCITY AND TEMPERATURE SPECTRA AND COSPECTRA IN THE GRADIENT SUBLAYER

For simplicity of theoretical analysis we consider here only pressure-gradient boundary layers in moving equilibrium conditions. The free-stream velocity U_∞ and kinematic pressure gradient γ are supposed to vary slowly enough with the coordinate x for the boundary layer to adjust to these variations, and its structure at any value of x depends essentially on the relevant local parameters (at the same x) only, not on the upstream history of the flow.

Let us consider the longitudinal (x-direction) spectra $E_i(k)$, where $i = u, v, w, t$, in the gradient layer (Fig. 1) of the developed boundary layer with heat transfer. Five different length-scales affect different ranges of wave number k—see Fig. 2, where δ and H are assumed to be of the same order of magnitude. In the small scale range $k \gg y^{-1}$ the size of the corresponding turbulent disturbances is much smaller than the distance from the wall y, hence here the spectra have a universal form if Kolmogorov scaling is used

$$E_i(k) = l_K v_K^2 \eta_i(kl_K),$$
$$E_t(k) = l_t t_K^2 \eta_t(kl_t, Pr) \quad \text{for} \quad k \gg y^{-1} \qquad (3)$$

where $i = u, v, w$, and $l_K = (\nu^3/\varepsilon)^{1/4}$, $l_t = l_K\ Pr^{-3/4}$, $v_K = (\nu\varepsilon)^{1/4}$ and $t_K = (N^2\nu/\varepsilon)^{1/4}$ are Kolmogorov's scales for viscous and diffusion lengths, velocity and temperature, while ε is the mean energy dissipation rate, N is the rate of dissipation for $\langle t^2\rangle/2$, and η_i, η_t are universal functions. Note that in the gradient sublayer

$$\varepsilon = a_\varepsilon \gamma^{3/2} y^{1/2}$$
$$N = a_N Q^2 \gamma^{-1/2} y^{-3/2} \qquad (4)$$

where a_ε and a_N are universal constants (see ref. [4]). Therefore, if $\delta_p \ll y \ll \delta$, then

$$l_K = a_\varepsilon^{-1/4}\gamma^{-3/8}\nu^{3/4}y^{-1/8} \quad l_t = a_\varepsilon^{-1/4}\gamma^{-3/8}\chi^{3/4}y^{-1/8}$$
$$v_K = \nu/l_K = a_\varepsilon^{1/4}\gamma^{3/8}\nu^{1/4}y^{1/8}$$
$$t_K = a_\varepsilon^{-1/4}a_N^{1/2}Q\gamma^{-5/8}\nu^{1/4}y^{-7/8}.$$

Another scaling is appropriate for the range $\delta^{-1} \ll k \ll l_K^{-1}$. Here γ and Q are the main parameters affecting the statistical regime of turbulent fluctuations. Therefore, y is the only length scale, $(\gamma y)^{1/2}$ is the only velocity scale and $Q(\gamma y)^{-1/2}$ is the only temperature scale. It follows from this that in the mesoscale wave number range

$$E_i(k) = \gamma y^2 \psi_i(ky)$$

$$E_t(k) = Q^2\gamma^{-1}\psi_t(ky) \quad \text{for} \quad y/\delta \ll ky \ll y/l_K \quad (5)$$

where $\psi_1 = \psi_u$, $\psi_2 = \psi_v$, $\psi_3 = \psi_w$ and ψ_t are some new universal functions.

The third wave number range, where spectral shapes are universal for special scaling, is the large-scale range of very small values of k corresponding to large-size turbulent disturbances with sizes of the order of the boundary layer thickness δ, H. The scales for length, velocity and temperature appropriate in this range are δ, $(\gamma\delta)^{1/2}$ and $Q(\gamma\delta)^{-1/2}$, respectively. This implies that

$$E_i(k) = \gamma\delta^2\phi_i(k\delta)$$

$$E_t(k) = Q^2\gamma^{-1}\phi_t(k\delta) \quad \text{for} \quad k \ll y^{-1}. \quad (6)$$

As was shown in another connection in ref. [15], this part of the spectrum, which describes the contribution of large-scale organized structures, sometimes plays a very important role. In particular, it determines the values of variances of horizontal wind fluctuations near the ground on hot summer days.

Let us now assume that there are two overlapping ranges where equations (3), (5) and, respectively, (5), (6), are valid simultaneously. In the first of these ranges we obtain

$$(\gamma^{-1}y^{-1/3}k^{5/3})E_i(k) = a_\varepsilon^{2/3}(kl_K)^{5/3}\eta_i(kl_K)$$

$$= (ky)^{5/3}\psi_i(ky) = a_i = \text{const} \quad (7a)$$

where $a_1 = a_u$, $a_2 = a_v$, $a_3 = a_w$ must be constant (since the arguments kl_K and ky are different and can change independently). The length of this region is determined by the inequalities $l_K^{-1} \gg k \gg y^{-1}$ and here

$$\psi_i(ky) = a_i(ky)^{-5/3} \quad \text{and} \quad \eta_i(kl_K) = a_i''(kl_K)^{-5/3}$$

$$a_i'' = a_i a_\varepsilon^{-2/3}. \quad (7b)$$

This range is the well-known Kolmogorov's inertial range. Its upper limit is given by $k = i_4/l_K$ where i_4 is a constant. The function $\eta_i(kl_K)$ at $kl_K = i_4$ begins to deviate from equation (7b). The lower wave number limit is equal $k = i_3/y$, where i_3 is a value of ky at which the function ψ_i begins to deviate from equation (7b). Naturally, the constants i_3 and i_4 can be different for $i = u, v, w$.

Similarly we can get a temperature spectrum in the overlapping range of Kolmogorov and mesoscale scalings (this range is nothing more than the inertial-convective wave number range). Here

$$[Q^{-2}\gamma(ky)^{5/3}]E_t(k) = a_\varepsilon^{-1/3}a_N(kl_K)^{5/3}\eta_t(kl_K, Pr)$$

$$= (ky)^{5/3}\psi_t(ky) = a_t = \text{const}$$

$$\text{for} \quad t_4(Pr)/l_K \leqslant k \leqslant t_3/y. \quad (8)$$

The second range, where all the spectral laws have quite simple forms, is the overlapping range of the low wave number and mesoscale k scalings, where equations (5) and (6) are simultaneously valid. Here

$$(\gamma^{-1}k^2)E_i(k) = (k\delta)^2\phi_i(k\delta)$$

$$= (ky)^2\psi_i(ky) = A_i = \text{const}$$

$$\text{for} \quad \delta^{-1} \ll k \ll y^{-1} \quad (9)$$

$$(Q^{-2}\gamma)E_t(k) = \phi_t(k\delta) = \psi_t(ky) = A_t = \text{const}$$

$$\text{for} \quad \delta^{-1} \ll k \ll y^{-1}. \quad (10)$$

Therefore, in this overlapping range, if it exists, the '-2 power law' must be valid for the velocity spectra

$$\phi_i(k\delta) = A_i(k\delta)^{-2} \quad \text{and} \quad \psi_i(ky) = A_i(ky)^{-2}$$

$$\text{for} \quad i_1/\delta \leqslant k \leqslant i_2/y \quad (9a)$$

and the 'constant law' must be valid for a temperature spectrum

$$\phi_t(k\delta) = A_t \quad \text{and} \quad \psi_t(ky) = A_t$$

$$\text{for} \quad t_1/\delta \leqslant k \leqslant t_2/y \quad (10a)$$

in the gradient sublayer $\delta_p \ll y \ll \delta$.

The laws (9a) and (10a) were obtained (in another way) and compared with the data in refs. [4, 10]. It was shown that the experimental data [3, 12–14] confirm the existence of the range where the '-2 power law' is valid and show that

$$A_u \cong 1.2\text{–}1.6 \quad A_v \cong 1.4 \quad A_t \cong 2.5\text{–}4. \quad (11a)$$

For the convective-inertial subrange of k values the data imply that

$$a_u \cong 0.9 \quad a_v \cong 1\text{–}1.2 \quad a_t \cong 0.5. \quad (11b)$$

If we take the most reliable [16] values of the Kolmogorov and Obukhov–Corrsin constants $\alpha_u \cong 0.5$ and $\alpha_t \cong 0.7$ entering '$-5/3$ power laws' for one-dimensional spectra

$$E_u(k) = \alpha_u\varepsilon^{2/3}k^{-5/3} \quad E_v(k) = (4\alpha_u/3)\varepsilon^{2/3}k^{-5/3}$$

$$\text{and} \quad E_t(k) = \alpha_t N\varepsilon^{-1/3}k^{-5/3}$$

we can calculate from equation (11b) the values of the constants a_ε and a_N in equations (4)

$$a_\varepsilon \cong 1.8\text{–}2.4 \quad \text{and} \quad a_N \cong 0.8\text{–}1 \quad (11c)$$

and evaluate Kolmogorov's scales l_K, l_t v_K, t_K in the gradient sublayer.

Combining equations (3) and (5)–(10) one can obtain the following model for velocity and temperature spectra in the gradient sublayer of a retarded turbulent boundary layer:

$$E_i(k) = \begin{cases} \gamma\delta^2\phi_i(k\delta) & \text{for } 0 < k < i_1/\delta \\ A_i\gamma k^{-2} & \text{for } i_1/\delta < k < i_2/y \\ \gamma y^2\psi_i(ky) & \text{for } i_2/y < k < i_3/y \\ a_i\gamma y^{1/3}k^{-5/3} & \text{for } i_3/y < k < i_4/l_K \\ l_K v_K^2 \eta_i(kl_K) & \text{for } i_4/l_K < k < \infty \end{cases} \quad (12)$$

and

$$E_t(k) = \begin{cases} Q^2\gamma^{-1}\phi_t(kH) & \text{for } 0 < k < t_1/H \\ A_t Q^2\gamma^{-1} & \text{for } t_1/H < k < t_2/y \\ Q^2\gamma^{-1}\psi_t(ky) & \text{for } i_2/y < k < i_3/y \\ a_t Q^2\gamma^{-1}(ky)^{-5/3} & \text{for } t_3/y < k < t_4(Pr)/l_K \\ l_K t_K^2 \eta_t(kl_K, Pr) & \text{for } t_4(Pr)/l_K < k < \infty \end{cases} \quad (13)$$

where $t_4(Pr)$ is a function of $Pr = \nu/\chi$.

With the aid of equation (12) the variance σ_i^2 can easily be calculated:

$$(\sigma_i/u_*)^2 = u_*^{-2}\int_0^\infty E_i(k)\,dk = I_1(\delta/\delta_p) + I_2(y/\delta_p) + I_3(y^{1/3}l_K^{2/3}/\delta_p)$$

or $\sigma_i^2/\gamma y = I_1(\delta/y) + I_2 + I_3(l_K/y)^{2/3}$

where I_1, I_2 and I_3 are three constants

$$I_1 = \int_0^{i_1}\phi_i(x)\,dx + A_i/i_1$$

$$I_2 = \int_{i_2}^{i_3}\psi_i(x)\,dx - A_i/i_2 + 1.5a_i i_3^{-2/3}$$

$$I_3 = a_\varepsilon^{2/3}\int_{i_4}^\infty \eta_i(x)\,dx - 1.5a_i i_4^{-2/3}.$$

The factors (δ/y), 1 and $(l_K/y)^{2/3}$ are quite different because $y \gg l_K$ and for a non-separated boundary layer in a gradient sublayer $\delta \gg y \gg \delta_p$ (see Fig. 1).

The values of coefficients I_1 and I_2 can be approximately evaluated with the aid of a simple model which uses the following assumptions: $\phi_i(k\delta) \to C_i$ = constant at $k\delta \to 0$; neglect the transition zone between validity ranges for -2 and $-5/3$ laws; and supposes that $i_4 = \infty$ (i.e. the simplified model neglects the dissipation range):

$$E_i(k) = \begin{cases} C_i\gamma\delta^2 & \text{for } 0 < k < i_1/\delta \\ A_i\gamma k^{-2} & \text{for } i_1/\delta < k < i_2/y \\ a_i\gamma y^{1/3}k^{-5/3} & \text{for } i_3/y < k < \infty. \end{cases} \quad (14)$$

It follows from the continuity of spectra that $i_1 = (A_i/C_i)^{1/2}$, $i_2 = i_3 = (A_i/a_i)^3$. Then

$$I_1 = 2(A_iC_i)^{1/2} \quad I_2 = 0.5(a_i^3/A_i^2).$$

In the same way it follows from equation (13) that

$$(\sigma_t/t_*)^2 = (u_*/Q)^2\int_0^\infty E_t(k)\,dk = T_1(\delta_p/\delta) + T_2(\delta_p/y) + T_3(\delta_p/y)(l_K/y)^{2/3}$$

$$\sigma_t^2/(Q^2/\gamma y) = T_1(y/\delta) + T_2 + T_3(l_K/y)^{2/3}$$

where

$$T_1 = \int_0^{t_1}\phi_t(x)\,dx + A_t t_1$$

$$T_2 = \int_{t_2}^{t_3}\psi_t(x)\,dx - A_t t_2 + 1.5a_t t_3^{-2/3}$$

$$T_3 = a_N a_\varepsilon^{-1/3}\int_{t_4}^\infty \eta_t(x)\,dx - 1.5a_t t_4^{-2/3}.$$

The simplified model of the form (13)

$$E_t(k) = \begin{cases} Q^2\gamma^{-1}A_t & \text{for } 0 < k < t_2/y \\ a_t Q^2\gamma^{-1}(ky)^{-5/3} & \text{for } t_3/y < k < \infty \end{cases} \quad (15)$$

where the spectrum continuity implies that $t_2 = t_3 = (a_t/A_t)^{3/5}$, $C_t = A_t$, $T_1 = T_3 = 0$, $T_2 = 2.5a_t(A_t/a_t)^{2/5}$ gives the result

$$(\sigma_t/t_*)^2 \cong 2.5a_t^{3/5}A_t^{2/5}Y^{-1/2}.$$

As to the cospectra E_{uv}, E_{ut} and E_{vt}, they are described in the overlapping range of low wave-number and mesoscale k scalings by the equations

$$E_{uv}(k) = A_{uv}\gamma k^{-2} \quad E_{ut}(k) = A_{ut}Qk^{-1}$$

$$E_{vt}(k) = A_{vt}Qk^{-1}. \quad (16)$$

As it was shown in ref. [4], the equations for $E_{uv}(k)$ and $E_{vt}(k)$ agree satisfactorily with the experimental data from ref. [3] (the cospectrum E_{ut} was not measured in ref. [3]).

Assuming, as is often done (see, e.g. refs. [17, 18]), that cospectra fall off as $k^{-7/3}$ in the inertial range and neglecting the dissipation range, we can propose for the cospectra the following model:

$$E_{uv}(k) = \begin{cases} \gamma\delta^2\phi_{uv}(k\delta) & \text{for } 0 < k < uv_1/\delta \\ A_{uv}\gamma k^{-2} & \text{for } uv_1/\delta < k < uv_2/y \\ \gamma y^2\psi_{uv}(ky) & \text{for } uv_2/y < k < uv_3/y \\ a_{uv}\gamma y^{-1/3}k^{-7/3} & \text{for } uv_3/y < k < \infty \end{cases} \quad (17)$$

and

$$E_{it}(k) = \begin{cases} QH\phi_{it}(kH) & \text{for} \quad 0 < k < it_1/H \\ A_{it}Qk^{-1} & \text{for} \quad it_1/H < k < it_2/y \\ Qy\psi_{it}(ky) & \text{for} \quad it_2/y < k < it_3/y \\ a_{it}Qy^{-4/3}k^{-7/3} & \text{for} \quad it_3/y < k < \infty \end{cases}$$

$$i = u, v \quad (18)$$

so we have

$$\langle -uv \rangle / u_*^2 = u_*^{-2} \int_0^\infty E_{uv}(k)\,\mathrm{d}k$$

$$= UV_1(\delta/\delta_p) + UV_2(y/\delta_p)$$

$$\langle vt \rangle / Q = Q^{-1} \int_0^\infty E_{vt}(k)\,\mathrm{d}k = VT_1 + A_{vt}\ln(H/y)$$

$$\langle ut \rangle / Q = Q^{-1} \int_0^\infty E_{ut}(k)\,\mathrm{d}k = UT_1 + A_{ut}\ln(H/y)$$

where

$$UV_1 = \int_0^{uv_1} \phi_{uv}(x)\,\mathrm{d}x + A_{uv}/uv_1$$

$$UV_2 = \int_{uv_2}^{uv_3} \psi_{uv}(x)\,\mathrm{d}x - A_{uv}/uv_2 + 0.75a_{uv}uv_3^{-4/3}$$

$$VT_1 = \int_0^{vt_1} \phi_{vt}(x)\,\mathrm{d}x + A_{vt}\ln(vt_2/vt_1)$$

$$+ \int_{vt_2}^{vt_3} \phi_{vt}(x)\,\mathrm{d}x + 0.75a_{vt}vt_3^{-4/3}$$

$$UT_1 = \int_0^{ut_1} \phi_{ut}(x)\,\mathrm{d}x + A_{ut}\ln(ut_2/ut_1)$$

$$+ \int_{ut_2}^{ut_3} \phi_{ut}(x)\,\mathrm{d}x + 0.75a_{ut}ut_3^{-4/3}.$$

If it is supposed that $\phi_\alpha(k\delta) = C_\alpha$, $\alpha_2 = \alpha_3$ for $\alpha = uv$, vt and ut, then, due to spectra continuity:

$$uv_1 = (A_{uv}/C_{uv})^{3/4} \quad uv_3 = (a_{uv}/A_{uv})^3$$

$$vt_1 = A_{vt}/C_{vt} \quad vt_3 = (a_{vt}/A_{vt})^{3/4}$$

$$ut_1 = A_{ut}/C_{ut} \quad ut_3 = (a_{ut}/A_{ut})^{3/4}$$

and, according to the simple models considered,

$$\langle -uv \rangle / u_*^2 = 2(A_{uv}C_{uv})^{1/2}(\gamma\delta/u_*^2)$$

$$-0.25(A_{uv}^4/a_{uv}^3)(\gamma y/u_*^2) \quad (19)$$

$$\langle vt \rangle / Q = A_{vt}[1.75 + \ln(a_{vt}^{3/4}C_{vt}/A_{vt}^{7/4})]$$

$$+ A_{vt}\ln(H/y) \quad (20)$$

$$\langle ut \rangle / Q = A_{ut}[1.75 + \ln(a_{ut}^{3/4}C_{ut}/A_{ut}^{7/4})]$$

$$+ A_{ut}\ln(H/y). \quad (21)$$

Table 1. The points of spectral measurements in ref. [3]

No.	y [mm]	y_+	y/δ	y/H	Y
1	1.5	28	0.016	0.022	0.8
2	4.0	75	0.043	0.059	2.1
3	10.0	190	0.11	0.15	5.2
4	40.0	750	0.43	0.59	21

3. COMPARISON WITH EXPERIMENT

3.1. *Moving equilibrium boundary layers*

Let us now compare the derived formulas with measured values of the spectra $E_i(k)$, $i = u, v, w, t$ and cospectra $E_{ij}(k)$, $E_{it}(k)$ in a moving-equilibrium decelerated boundary layer on a heated plate studied by Roganov [3]. In this experiment $Z = \delta/\delta_p = \gamma\delta/u_*^2 \cong 45$ and $S = \delta_p/\delta_v = u_*^3/\gamma\nu \cong 35$ for the cross-section at $x = 955$ mm, where the measurements were made. These values of Z and S are large enough to believe that the gradient sublayer in the boundary layer exists and is easily observable. Though there are some differences between measured thicknesses $\delta \cong 93.3$ mm and H $\cong 68$ mm, we can at first not take them into account because, as was explained above, they do not affect noticeably the characteristics of turbulence in the gradient sublayer. The spectra in ref. [3] were measured at four points (see Table 1). Two of these points, where $y/\delta_p = 0.8$ and 21, lie approximately outside or close to the boundaries of the gradient sublayer.

Spectra $E_u(k)$ of longitudinal velocity fluctuations measured in ref. [3] agree satisfactorily with the proposed model (12), where $i = u$. Figure 3(a) represents the function $E_uk^2/\gamma = f(k\delta)$ which, according to equation (12), is equal to $A_u =$ const in the range where the -2 power law is valid. The figure shows that four non-dimensional $E_u(k)k^2/\gamma$ spectra are close to each other in the low wave number range and, at very low values of k, these spectra become independent on k. Therefore

$$\phi_u(k\delta) \to C_u = \text{const} \quad E_u(k) = C_u\gamma\delta^2$$

$$C_u \cong 0.08 \quad \text{for}\, k\delta < 1.$$

There is a rather wide transition zone between the range of constancy for $E_u(k)$ and the validity range of the -2 power law but the low wave number parts of all the spectra, including the domain of mesoscale values of k, can be described by a simple interpolation formula $E_u(k) = A_u\gamma\delta^2/[A_u/C_u + 3(k\delta) + (k\delta)^2]$. At the same time the transition zone between the validity ranges for the -2 and $-5/3$ power laws proves to be so narrow (see also ref. [4]) that it is possible to assume that $u_2 = u_3$ in equation (12). Therefore, if we neglect the small amount of very high wave number energy, then

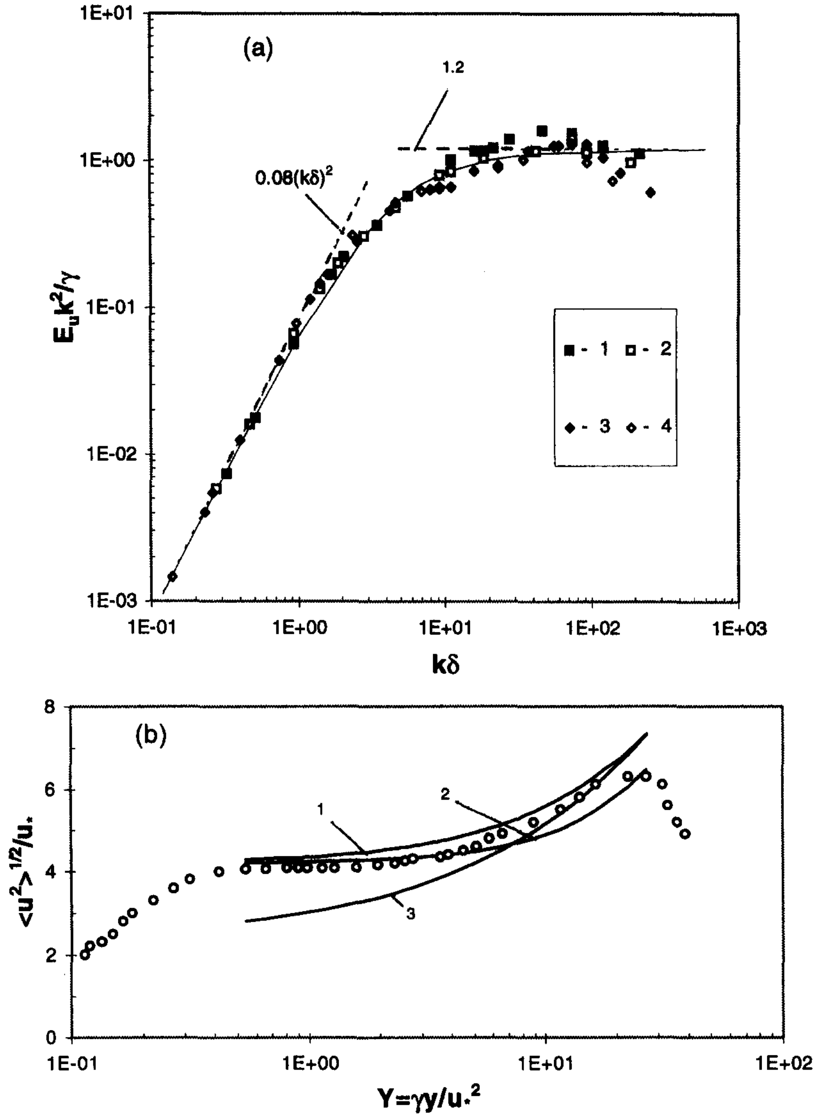

Fig. 3. (a) The longitudinal spectrum of u-fluctuations [3] in the gradient sublayer (points 2 and 3—see Table 1) and close to its boundaries (points 1 and 4) normalized by γ and δ. The solid line corresponds to the interpolation formula on the upper line of the right-hand side [equation (22a)], and the dashed lines correspond to the limiting relations for $k\delta \gg 1$ and $k\delta \ll 1$. (b) The profile of normalized standard deviation for u-fluctuations [3]. (1) Calculations based on equation (22c); (2) calculations based on the simplified formula (24); (3) calculations based on the interpolation formula (23a).

$$E_u(k) = \begin{cases} A_u\gamma\delta^2/[A_u/C_u+3(k\delta)+(k\delta)^2] & \text{for} \quad 0 < k < u_2/y \\ a_u\gamma y^{1/3}k^{-5/3} & \text{for} \quad u_3/y < k < \infty \end{cases} \tag{22a}$$

where according to Fig. 3(a) and equations (11a) and (11b) (see Fig. 14 in ref. [4])

$$C_u \cong 0.08 \quad A_u \cong 1.2 \quad a_u \cong 0.9 \quad u_2 \cong u_3 \cong 1. \tag{22b}$$

These results imply the following equation:

$$(\sigma_u/u_*)^2 = u_*^{-2}\int_0^\infty E_u(k)\,\mathrm{d}k$$

$$= A_u Z\frac{2}{\sqrt{51}}\left[\tan^{-1}\left(\frac{2Z/Y+3}{\sqrt{51}}\right) - \tan^{-1}\left(\frac{3}{\sqrt{51}}\right)\right] + 1.5a_u Y \tag{22c}$$

which is compared with the experimental data [3] in Fig. 3(b). There is also a curve in this figure that meets the first of the formulas

$$(\sigma_u/u_*)^2 = 1.3(4+2(\sqrt{Y})+Y) \quad (23a)$$

$$(\sigma_v/u_*)^2 = 1+(\sqrt{Y})/3+Y/3 \quad (23b)$$

$$(\sigma_w/u_*)^2 = 3+(\sqrt{Y})+0.8Y \quad (23c)$$

proposed in ref. [19] (see also ref. [20]) on the basis of an interpolation between near separated ($Y \to \infty$) and constant-pressure ($Y \to 0$) turbulent wall flows. The comparison shows that the relation (22c) agrees better with the experimental data analyzed and in accordance with a remark in ref. [19], a value of $Z = \delta/\delta_p = \gamma\delta/u_*^2$ noticeably affects the value of σ_u/u_*.

The relation (22c) can be simplified if we take into account that in the gradient sublayer, where according to ref. [10] $u_*^2/\gamma \leqslant y \leqslant 0.3\delta$, i.e. $Z/Y = \delta/y > 3$, the argument of $\tan^{-1}$ is large enough to suppose that $\tan^{-1}(\ldots) \cong \pi/2$. Then

$$(\sigma_u/u_*)^2 \cong 0.4Z+1.35Y \quad (24)$$

[compare with the results of calculations by (23a) in Fig. 3(b)].

The normalized spectra $E_v(k)/\gamma\delta^2$ prove to be more sophisticated and do not coincide with each other at the low wave number range, as can be seen in Fig. 4(a). All spectra tend to C_v = const when $k\delta \to 0$ but, in a contradiction to equation (12), the value of this constant depends on y/δ_p even for $Y = 2.1$ and 5.2 inside the gradient sublayer. The spectrum model (12) is clearly valid only if there is enough energy in the low wave number range. For the vertical velocity spectrum $E_v(k)$ the energy range is much narrower than for horizontal velocities. Therefore, we should use the y instead of the δ scale, and we should change the first and the second lines in equation (12) for

$$E_v(k) = \begin{cases} yu_*^2\phi_v(ky) & \text{for} \quad 0 < k < i_1/y \\ A_v\gamma k^{-2} & \text{for} \quad i_1/y < k < i_2/y. \end{cases}$$

In Fig. 4(b) we can see that all spectral data in low k coincide with each other and an approximation

$$E_v(k) = \begin{cases} A_v yu_*^2/(A_v/C_v+(yu_*^2/\gamma)k^2) & \text{for} \quad 0 < k < v_2/y \\ a_v\gamma y^{1/3}k^{-5/3} & \text{for} \quad v_3/y < k < \infty \end{cases} \quad (25a)$$

can be used, where $v_2 = v_3$. According to the experimental data

$$C_v = 0.055^*Z \cong 2.5 \quad A_v \cong 1.2$$
$$a_v \cong 1 \quad v_2 = v_3 \cong 10 \quad (25b)$$

therefore

$$(\sigma_v/u_*)^2 = u_*^{-2}\int_0^\infty E_v(k)\,\mathrm{d}k = \sqrt{A_vC_v}\sqrt{Y}$$
$$\times \tan^{-1}(v_3\sqrt{(C_v/A_v)}/\sqrt{Y})+1.5a_vv_3^{-2/3}Y$$
$$= 0.26\sqrt{Z}\sqrt{Y}\tan^{-1}(2.1\sqrt{Z}/\sqrt{Y})+0.3Y \quad (25c)$$

which can be simplified if we suppose $v_3 \to \infty$

$$(\sigma_v/u_*)^2 \cong 0.4\sqrt{Z}\sqrt{Y} \quad (25d)$$

[compare with the results of calculations by equation (23b) shown in Fig. 4(c)].

It is worth noting here that if equation (6) proves to be inconsistent with the $E_v(k)$ spectrum then the existence of an overlapping range of low wave number scaling and mesoscale k scaling becomes doubtful and, thereafter, there is no basis for derivation of the -2 power law. In addition, it is difficult to distinguish the -2 power law from the nearby $-5/3$ law when the area of validity of these laws is rather narrow. From the other side, according to numerous experimental data, we should not expect a noticeable k range where $E_v(k) \sim k^{-5/3}$ for low Re number flows.

Let us now consider the spectrum $E_t(k)$. The corresponding experimental data more or less satisfactorily coincide with each other in the low wave number range and can be described by model (13)—see Fig. 5(a) where only data for points inside the gradient sublayer (for $Y = 2.1$ and 5.2) are used. We see that $E_t(k)\gamma/Q^2 \to C_t$ = const when $kH \to 0$. For all values of k, a simple approximation formula of the form

$$E_t(k) = A_tQ^2\gamma^{-1}/[A_t/C_t+A_t/a_t(ky)^{5/3}] \quad \text{for} \quad 0 < k < \infty \quad (26a)$$

can be used where according to equations (11a) and (11b)

$$C_t \cong A_t \cong 3 \quad \text{and} \quad a_t \cong 0.5. \quad (26b)$$

Therefore

$$(\sigma_t/t_*)^2 = (u_*/Q)^2\int_0^\infty E_t(k)\,\mathrm{d}k$$
$$= A_t^{2/5}a_t^{2/5}\frac{3\pi}{5\sin(3\pi/5)}Y^{-1} \cong 2/Y. \quad (26c)$$

This equation agrees satisfactorily with experimental data [see Fig. 5(b)].

In just in the same way we analyze the experimental data from ref. [3] related to cospectra of a temperature flux in the gradient sublayer [Fig. 6(a)]. They can be approximated by a simple formula

$$E_{vt}(k) = \begin{cases} A_{vt}QH/[(A_{vt}/C_{vt})^2+(kH)^2]^{1/2} & \text{for} \quad 0 < k < vt_3/y \\ a_{vt}Qy^{-4/3}k^{-7/3} & \text{for} \quad vt_3/y < k < \infty \end{cases} \quad (27a)$$

where according to ref. [3]

$$A_{vt} \cong 0.25 \quad a_{vt} \cong 0.6 \quad C_{vt} \cong 0.1 \quad \text{and} \quad vt_2 \cong 2. \quad (27b)$$

The approximation (27a) agrees with the spectrum model (18) and implies that

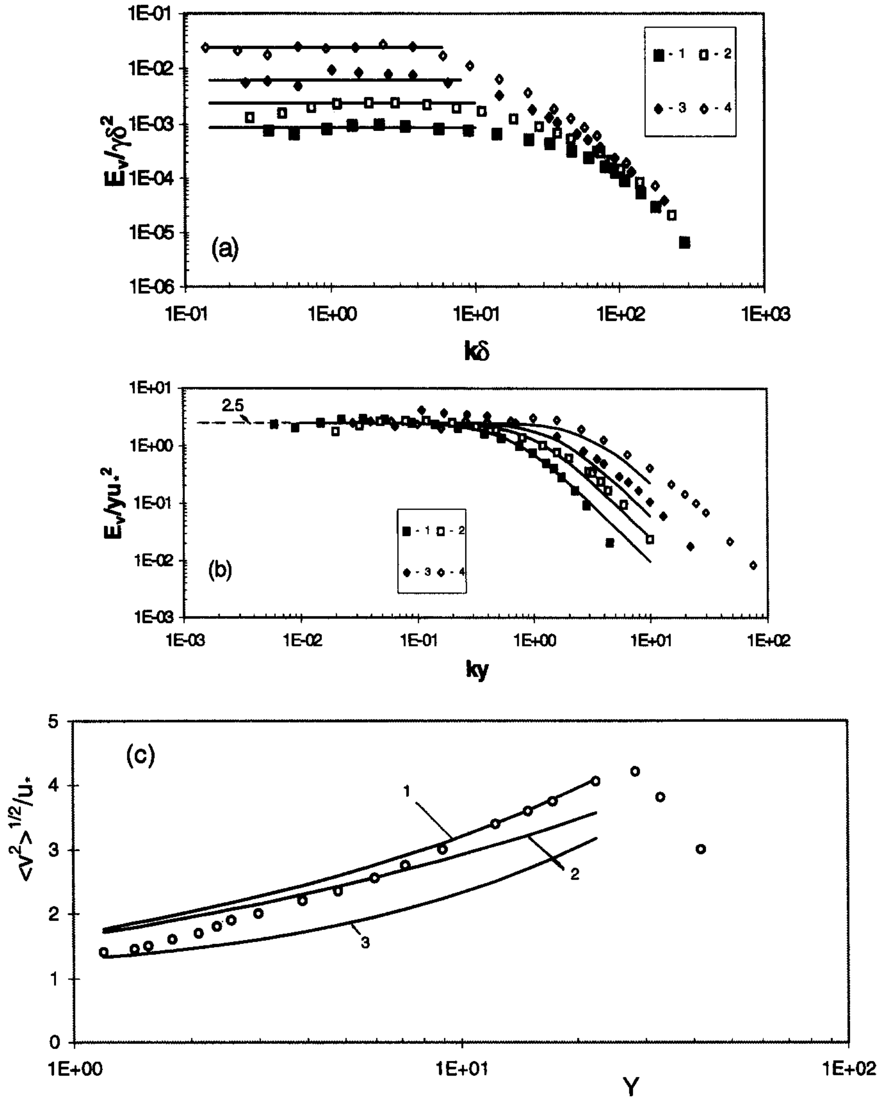

Fig. 4. (a,b) The longitudinal spectrum of normal velocity fluctuations [3] in the gradient sublayer (points 2 and 3—see Table 1) and close to its boundaries (points 1 and 4). (a) Spectra are normalized by γ and δ. The solid lines correspond to the relation $E_v(k) \propto \gamma\delta^2$. (b) Spectra are normalized by u_* and y. The solid line corresponds to the interpolation formula on the upper line of the right-hand side of equation (25a), and the dashed line corresponds to the limiting relations for $ky \ll 1$. (c) The profile of normalized standard deviation for v-fluctuations. (1) Calculations based on equation (25c); (2) calculations based on the simplified formula (25d); (3) calculations based on the interpolation formula (23b).

$$\langle vt\rangle/Q = A_{vt}\ln\{(vt_3/2)+\surd[(y/H)^2+(vt_3/2)^2]\} + 0.75a_{vt}vt_3^{-4/3} \cong 0.25\ln\{1+\surd[1+(y/H)^2]\} + 0.18+0.25\ln(H/y). \quad (27c)$$

The simplified model (20) gives

$$\langle vt\rangle/Q \cong 0.38+0.21\ln(H/y). \quad (27d)$$

Both models within the region of their validity agree quite satisfactorily with each other and with the experimental data in Fig. 6(b).

Like the case of spectra $E_v(k)$ the normalized cospectra of Reynolds stress $\langle -uv\rangle$ do not coincide in the low wave number range [Fig. 7(a)]. Taking into account that in the low wave number range the linear scales for horizontal and vertical fluctuations are δ and y, respectively, we can use a model with geometric mean linear-scale $\surd y\delta$ in the spectral model (17). According to data from ref. [3]

$$A_{uv} = 0.35 \quad C_{uv} = C''_{uv}Z \quad C''_{uv} \cong 0.14 \quad (28a)$$

and the empirical approximation

$$E_{uv}(k) = A_{uv}\gamma\delta y/(A_{uv}/C''_{uv}+y\delta k^2) \quad (28b)$$

agrees well enough with the experimental data [see

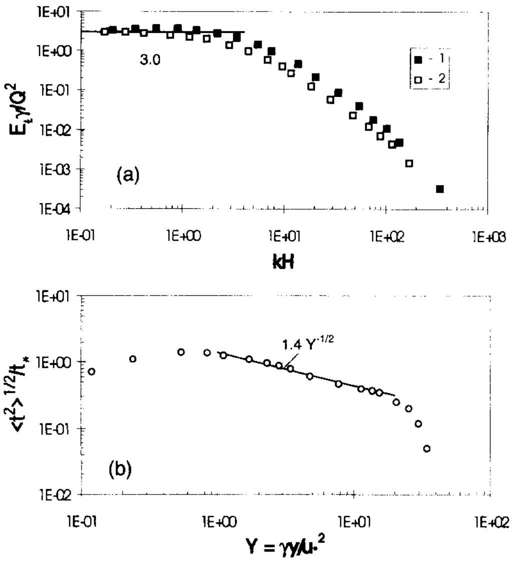

Fig. 5. (a) The longitudinal spectrum of temperature fluctuations [3] in the gradient sublayer (points 2 and 3 in Table 1) normalized by γ, Q and H. The solid line corresponds to the relation $E_t\gamma/Q^2 = C_t = \text{const.}$ (b) The profile of the normalized standard deviation for temperature fluctuations. The solid line corresponds to equation (26c).

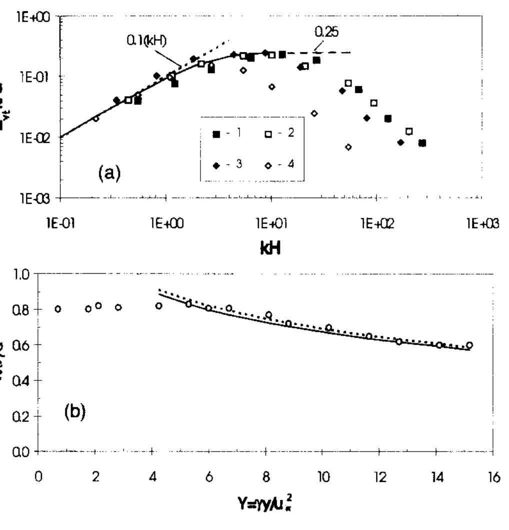

Fig. 6. (a) The longitudinal cospectrum of temperature flux fluctuations in the gradient sublayer normalized by γ, Q and H according to ref. [3]. The solid line corresponds to the interpolation formula on the upper line of the right-hand side of equation (27a). (b) The profile of normalized temperature flux in the gradient sublayer. The solid line corresponds to equation (27c).

Fig. 7(b)]. At the same time it proved to be impossible to determine a value of uv_3 where the experimental data begin to deviate from the $-5/3$ law to a $-7/3$ law according to the spectral model (18). Therefore, we use the relation (28b) to evaluate normalized Reynolds stresses

$$\langle -uv\rangle/u_*^2 = (\pi/2)(A_{uv}C''_{uv})^{1/2}Z^{1/2}Y^{1/2} \cong 0.35\sqrt{Z}\sqrt{Y} \tag{28c}$$

and compare it with experimental data [Fig. 7(c)]. The simplified model (19) with $uv_2 \to \infty$ gives a bit higher coefficient in equation (28c): $\langle -uv\rangle/u_*^2 \cong 0.44\sqrt{Z}\sqrt{Y}$.

Compared with the interpolation formula

$$\langle -uv\rangle/u_*^2 = 0.25(4+(\sqrt{Y})+Y) \tag{28d}$$

proposed in ref. [19] (see also ref. [20]) equation (28c) describes the experimental data better.

Like all other methods of predicting the characteristics of turbulent boundary layers, the formulas derived above contain a large degree of empiricism. To check the universality of the empirical constants in the proposed formulas we compared them with the experimental data [21], which became known to us when the present paper had already been finished and accepted for publication. Report [21] does not contain any spectral data but it includes unique measurements of one-point second-order moments in equilibrium flows with very high pressure gradients. Only strong adverse pressure gradient data in flow Nos. 6,7 with $Z \gg 1$ were used (see Table 2).

All experimental data and calculated results are summarized in Fig. 8. With the exception of u-fluctuations near the wall in the near separated flow No.7, where the difference between measured and calculated values of standard deviations reaches 40%, the experimental values of normal to the wall velocity and Reynolds stress fluctuations prove to agree well with the above equations.

3.2. *Non-equilibrium flows*

Although the investigation of the general case of non-equilibrium retarded boundary layers is beyond the scope of this paper, it is worth seeing how deviation from moving equilibrium conditions can distort the turbulent structure in the gradient sublayer, if it exists. Quite recently very accurate and detailed spectral measurements in non-equilibrium retarded turbulent flows have been accomplished [22]. They were used partially (see Table 3 where only the case $U_\infty = 30\ \text{m s}^{-1}$ was considered) to check the effect of deviation from equilibrium on the spectra and one-point moments.

In Fig. 9 it can be seen that the lack of equilibrium distorts the mesoscale energy containing parts of the spectra. Discrepancies are noticed in particular in the longitudinal spectra of the normal velocity and Reynolds stress fluctuations. At the same time the experimental spectra of u-fluctuations are not noticeably different from calculated ones, therefore it is not surprising that the proposed formula (22c) more or less agrees with the experiment even without equilibrium—see Fig. 10. In the cases of normal velocity and Reynolds stress fluctuations the agreement is much less satisfactory.

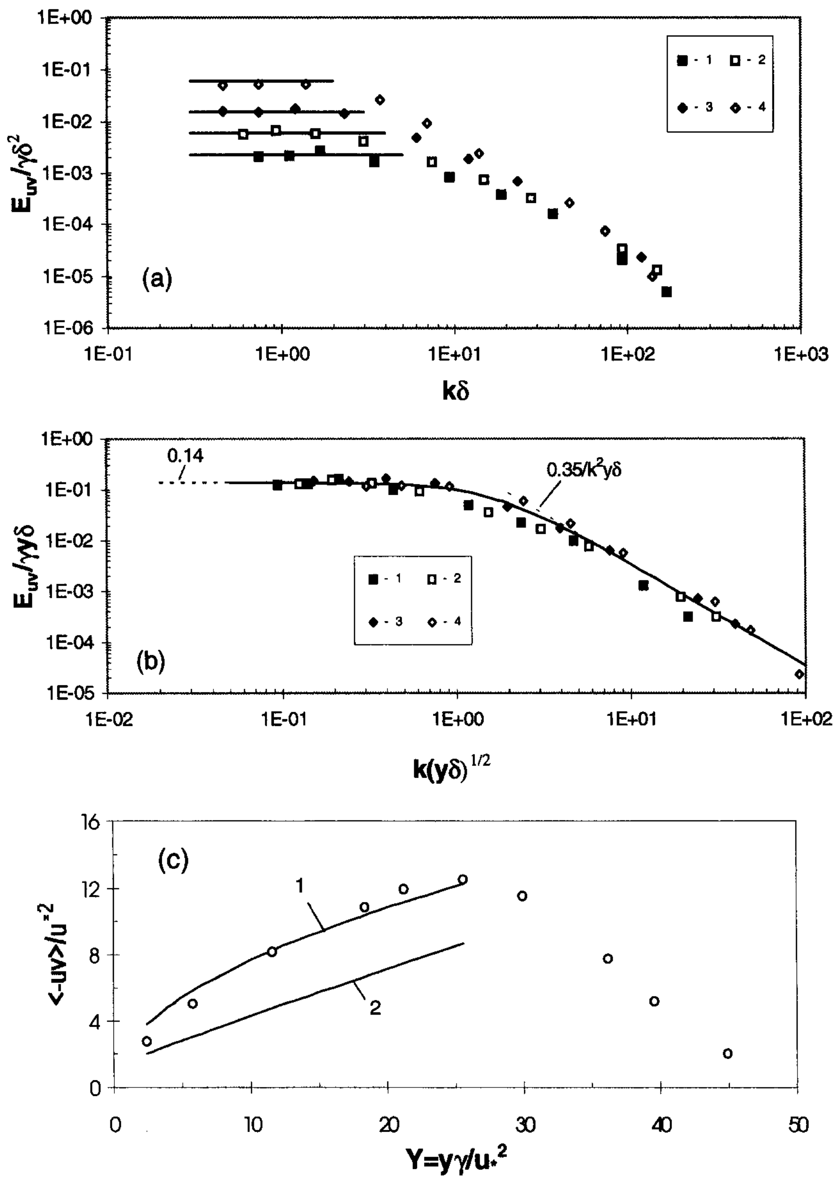

Fig. 7. (a,b) The longitudinal spectrum of Reynolds stress fluctuations [3] in the gradient sublayer. (a) Spectra are normalized by γ and δ. The solid line correspond to the relation $E_{uv}(k) \propto \gamma\delta^2$. (b) Spectra are normalized by γ and $\sqrt{\gamma\delta}$. The solid line corresponds to the interpolation formula (28b) and the dashed lines correspond to the limiting relations shown in the graph. (c) The profile of normalized Reynolds stress in the gradient sublayer [3]. (1) Calculations based on equation (28c); (2) calculations based on the interpolation formula (28d).

Table 2. Parameters of flows in ref. [23] used in the analysis

Flow No.	x [mm]	U_∞ [m s^{-1}]	δ [mm]	u_* [m s^{-1}]	γ [m s^{-2}]	S	Z
6	3858	22.30	151.2	0.518	47.3	196	26.6
7	3858	19.61	260.2	0.240	34.7	26.6	156.4

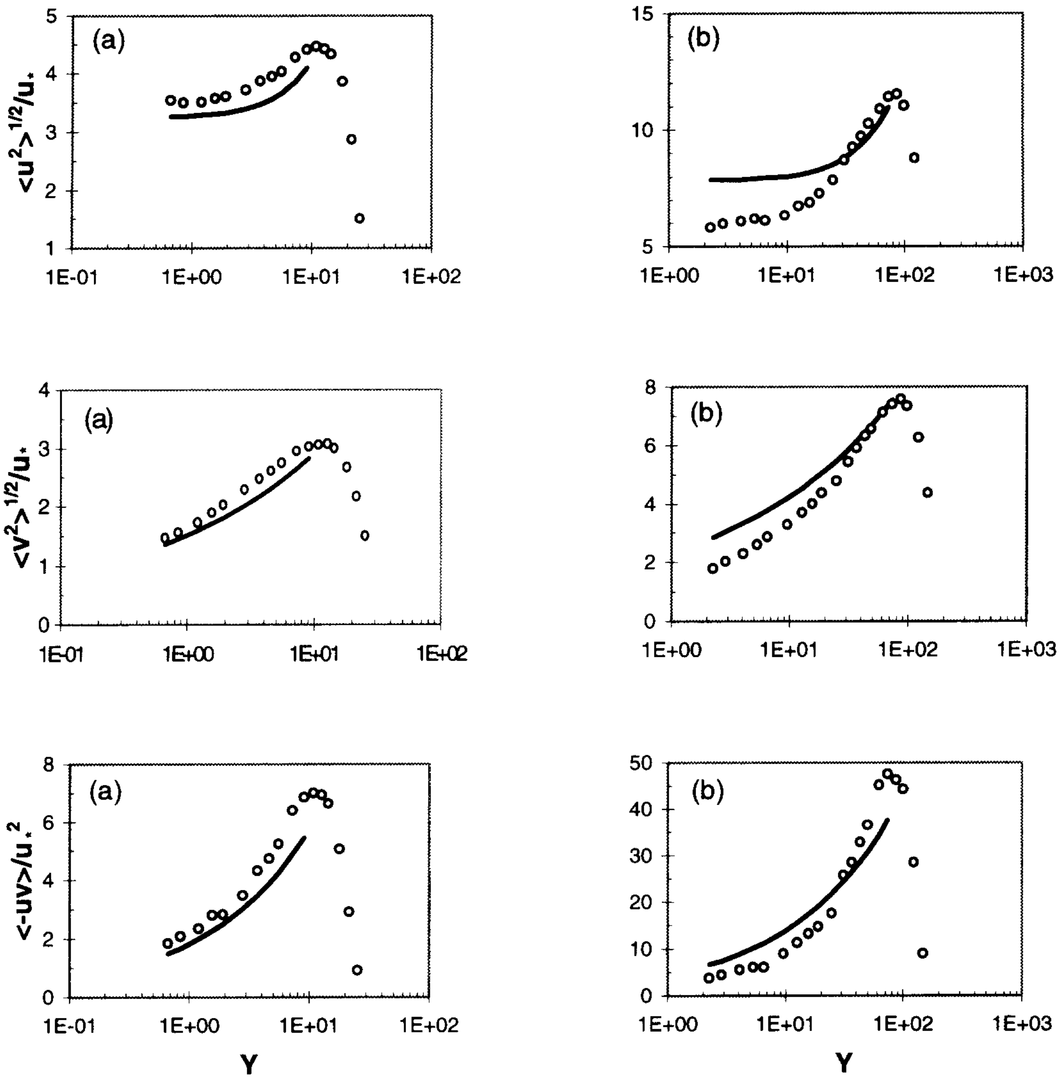

Fig. 8. Comparison of experimental data from ref. [21] with equation (22c) for profiles $\langle u^2\rangle^{1/2}/u_*$, equation (25c) for $\langle v^2\rangle^{1/2}/u_*$ and equation (28c) for Reynolds shear stress. (a) flow No.6; (b) flow No. 7.

4. CORRELATION FUNCTION IN THE GRADIENT SUBLAYER

The spectral results above can be used for finding longitudinal correlation (more precisely, auto-correlation) functions

$$\langle i(x+\Delta x, y, z)i(x, y, z)\rangle = B_i(\Delta x\,; y) \quad i = u, v, w$$

and symmetrized cross-correlation functions

$$B_{ij}(\Delta x\,; y) = \tfrac{1}{2}\langle i(x+\Delta x, y, z)j(x, y, z) + i(x, y, z)j(x+\Delta x, y, z)\rangle \quad i = u, v, w$$

of turbulent fluctuations within the gradient sublayer of retarded turbulent boundary layers. In fact, these functions are Fourier transforms of the corresponding longitudinal spectra and cospectra:

$$B_i(\Delta x\,; y) = \int_0^\infty \cos(k\Delta x)E_i(k\,; y)\,\mathrm{d}k \quad i = u, v, w, t \tag{29a}$$

$$B_{ij}(\Delta x\,; y) = \int_0^\infty \cos(k\Delta x)E_{ij}(k\,; y)\,\mathrm{d}k \quad i,j = u, v, w, t. \tag{29b}$$

There are some reasons why formulas deduced in such a way are less interesting and reliable than corresponding spectral equations. First of all, there are no data which we can use to obtain measured values of longitudinal correlation functions in decelerated boundary layers. Moreover, we must also note that our results are based on the assumptions that the

Table 3. Parameters of boundary layers in two stations in ref. [22] for the case $U_\infty = 30\ \mathrm{m\ s^{-1}}$

No.	x [mm]	U_∞ [m s^{-1}]	δ_H [mm]	u_* [m s^{-1}]	γ [m s^{-2}]	S	Z
1	2880	14.36	81.5	0.67	108.6	177	19.7
2	3080	14.99	92.5	0.60	104.9	129	27.2

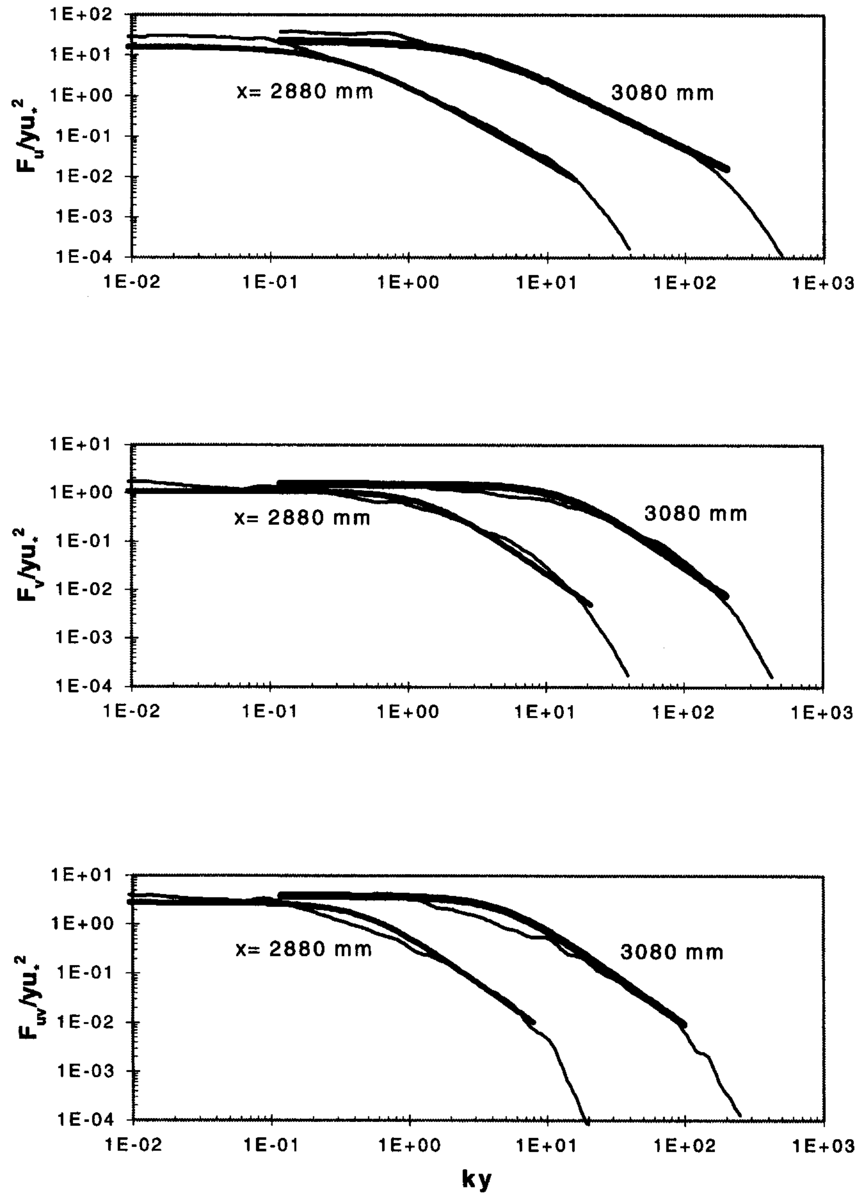

Fig. 9. Streamwise spectra in non-equilibrium retarded flow [22] (30 m s^{-1} flow case). The solid lines correspond to the interpolation formulas on the upper lines of the right-hand sides of equation (22a), (25a) and (28b).

turbulent structure in the gradient sublayer is determined mainly by the values of kinematic pressure gradient γ and temperature flux Q. Therefore we propose that all these parameters are approximately constant in the region of longitudinal spatial measurements. It is clear that these requirements, which are

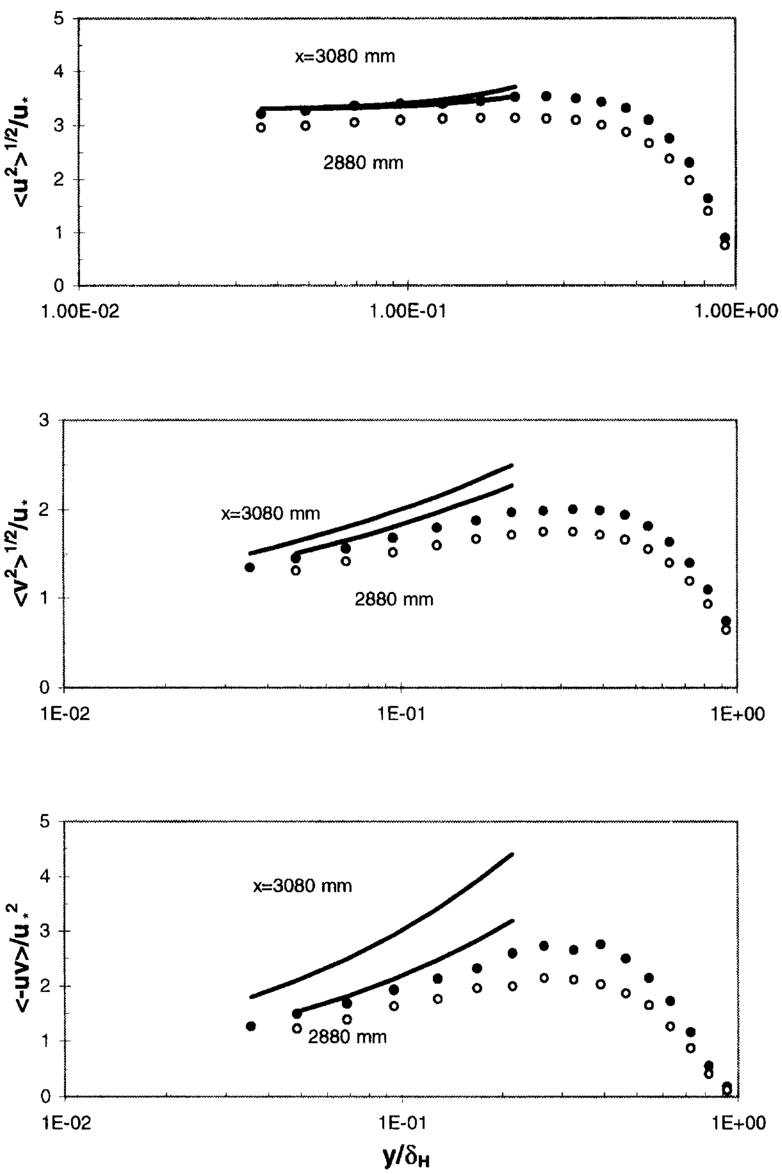

Fig. 10. Comparison of experimental data from ref. [22] with equation (22c) for profiles $\langle u^2\rangle^{1/2}/u_*$, equation (25c) for $\langle v^2\rangle^{1/2}/u_*$ and equation (28c) for Reynolds shear stress $\langle -uv\rangle/u_*^2$ for two stations: $x = 2880$ mm and $x = 3080$ mm.

included in the conditions for moving-equilibrium, restrict considerably the class of pressure-gradient boundary layers that can be used for verification of the given equations. [They are probably more appropriate to spatial transversal correlation functions $B_i(\Delta z; y)$ and $B_{ij}(\Delta z; y)$ in plain-parallel turbulent wall flows with longitudinal pressure gradient. All the above spectral results can be easily applied to the transversal spectra of turbulent velocity and temperature fluctuations, but we cannot use Taylor's hypothesis then, and therefore there are at present no experimental results which can be used to verify the conclusions related to transversal characteristics.] Nevertheless, it seems reasonable to consider briefly some results for longitudinal correlation functions to stimulate experimental measurements of these important statistical characteristics. Note in this respect that similarly derived equations in refs. [18, 23] for spatial correlation functions of surface-layer atmospheric turbulence proved to be helpful in micrometeorological studies.

In the gradient sublayer the spectra $E_i(k)$ and cospectra $E_{ij}(k)$, $i = u, v, w, t$ are given by equations (12), (13), (17) and (18). Let us begin with the autocorrelation functions for the very small longitudinal distance $\Delta x \leqslant l_K/i_4$. Since the wave numbers $k > 1/\Delta x$ are very large in this case, the contribution of the spectral range where $k\Delta x > 1$ to the integral on the right-hand side of equation (29a) is negligible, and we can replace $\cos(k\Delta x)$ in it by the two first term Taylor's expansion of this function. Then, using the well-known equations from the theory of locally isotropical turbulence (see, e.g. [11]), we obtain

$$B_i(\Delta x/y) = \sigma_i^2 - A_i(\Delta x/y)^2 \quad i = u, v, w, t \quad (30)$$

where $A_u = y^2\varepsilon/30\nu$, $A_v = A_w = y^2\varepsilon/15\nu$ and $A_t = y^2N/6\chi$.

Consider now the case where $\Delta x \gg l_K$. According to equation (12)

$$\begin{aligned} B_i(\Delta x) &= \sigma_i^2 - (\gamma\delta^2/\Delta x)\int_0^{i_1\Delta x/\delta}(1-\cos q)\phi_i\left(q\frac{\Delta x}{y}\right)\mathrm{d}q \\ &\quad - A_i\gamma\Delta x\int_{i_1\Delta x/\delta}^{i_2\Delta x/y}(1-\cos q)q^{-2}\,\mathrm{d}q \\ &\quad - (\gamma y^2/\Delta x)\int_{i_2\Delta x/y}^{i_3\Delta x/y}(1-\cos q)\psi_i\left(q\frac{\Delta x}{y}\right)\mathrm{d}q \\ &\quad - a_i\gamma y^{1/3}\Delta x^{2/3}\int_{i_3\Delta x/y}^{i_4\Delta x/l_K}(1-\cos q)q^{-5/3}\,\mathrm{d}q \\ &\quad - (l_K v_K^2/\Delta x)\int_{i_4\Delta x/l_K}^{\infty}(1-\cos q)\eta_i\left(q\frac{l_K}{\Delta x}\right)\mathrm{d}q \\ &= \sigma_i^2 - I_1 - I_2 - I_3 - I_4 - I_5 \end{aligned} \quad (31)$$

where I_1, I_2, I_3, I_4 and I_5 are the contributions of spectral subranges of low wave numbers ($0 < k < i_1/\delta$), wave numbers where the -2 power law is valid ($i_1/\delta < k < i_2/y$), intermediate wave numbers ($i_2/y < k < i_3/y$), wave numbers from the inertial interval ($i_3/y < k < i_4/l_K$) and dissipative-subrange wave numbers ($i_4/l_K < k < \infty$).

If $\Delta x < l_K/i_4$ then a lower limit of the integral I_5 is less than one and therefore all limits in I_1–I_4 are less than one. In this case the term I_5 plays the main role, i.e. the contribution of a dissipation-subrange wave number to B_i is the most important, and a spatial correlation function is described by equation (30).

For Δx belonging to the inertial interval, i.e. for $l_K < \Delta x < y$, we obtain

$$\begin{aligned} B_i(\Delta x/y) &= \sigma_i^2 - a_i\gamma y(\Delta x/y)^{2/3}[0.75\Gamma(1/3) \\ &\quad + O(\Delta x/l_K)^{-2/3} + O(\Delta x/y)^{4/3}] \\ &\cong \sigma_i^2 - 0.75\Gamma(1/3)a_i\gamma y(\Delta x/y)^{2/3} \quad i = u, v, w \end{aligned} \quad (32)$$

where Γ is the Gamma function. The main contribution to equation (31) is provided by the integral I_4 and estimated by equations (3.761.7), (8.354.2) and (8.357) from ref. [24]. The contributions of the dissipation spectrum subrange integral I_5 and I_3 plus the -2 power law integral I_2 are evaluated as $O[\gamma y(l_K/y)^{2/3}]$ and $O[\gamma y(\Delta x/y)^2]$ and prove to be much less than $(\Delta x/y)^{2/3}$ for $l_K/i_4 < \Delta x < y/i_3$. This result is equivalent to the 2/3 power law for velocity and temperature structure functions [11].

Let us assume now that $y < \Delta x < \delta$. Here the main contribution to equation (32) is provided by the meso-scale wave number integral I_2, and integrals I_1, I_2, I_3 can be estimated with some algebra from equations (3.761.7), (8.230.1), (8.232.1), (8.354.2) and (8.357) in ref. [24] and equation (9.8.10) in ref. [25]. It leads to the linear correlation function

$$\begin{aligned} B_i(\Delta x/y) &= \sigma_i^2 - A_i\gamma y(\Delta x/y)[\pi/2 - (y/\Delta x)/i_2 \\ &\quad + O(y/\Delta x)^2 + O(\Delta x/\delta)] \\ &\quad - a_i\gamma y^{1/3}\Delta x^{2/3}[1.5(i_2\Delta x/y)^{-2/3} \\ &\quad - 1.5(i_3\Delta x/l_K)^{-2/3}] \\ &\cong \sigma_i^2 - \gamma y[1.5a_i i_2^{-2/3} - A_i/i_2] \\ &\quad - A_i(\pi/2)\gamma y(\Delta x/y) \quad i = u, v, w. \end{aligned} \quad (33)$$

The accuracy of this formula is $O[\gamma y(y/\Delta x)]$ and $O[\gamma\delta(\Delta x/\delta)]$.

It is not difficult to estimate the correlation functions at $\Delta x > \delta$ if we use the low wave number spectral regions $k < i_1/\delta$ or the approximation formulas (22a) and (25a) for $E_u(k)$ and $E_v(k)$ in the range of mesoscale and low k domain but, as stated above, the validity of the experimental correlation data in the region $\Delta x > \delta$ is doubtful.

Similarily we can also use equations (13) to evaluate a correlation function for temperature fluctuation in the gradient sublayer:

$$B_t(\Delta x/y) \cong \sigma_t^2 - 0.75\Gamma(1/3)a_t(Q^2/\gamma y)(\Delta x/y)^{2/3} \quad \text{for} \quad l_K/t_4 < \Delta x < y/t_3 \quad (34)$$

with accuracy $O[(Q^2/\gamma y)(l_K/y)^{2/3}]$ and $O[(Q^2/\gamma y)(\Delta x/y)^2]$ and

$$\begin{aligned} B_t(\Delta x/y) &= \sigma_t^2 - (Q^2/\gamma y)(A_t t_2 - 1.5a_t t_1^{-2/3}) \\ &\quad - A_t(Q^2/\gamma y)(y/\Delta x)\sin(t_2\Delta x/y) \\ &\quad \text{for} \quad y/t_2 < \Delta x < H/t_1 \end{aligned} \quad (35)$$

with accuracy $O[(Q^2/\gamma H)(\Delta x/H)^2]$ and $O[(Q^2/\gamma y)(y/\Delta x)]$.

Cross-correlation functions for Reynolds stresses $\langle -uv\rangle$ follow from equation (17):

$$B_{uv}(\Delta x/y) \cong \langle -uv\rangle - \tfrac{9}{16}\Gamma(1/3)\gamma y a_{uv}(\Delta x/y)^{4/3} \quad \text{for} \quad \Delta x < y/uv_3$$

$$\begin{aligned} B_{uv}(\Delta x/y) &\cong \langle -uv\rangle - \gamma y[0.75a_{uv}uv_3^{-4/3} \\ &\quad - A_{uv}/uv_2] - A_{uv}(\pi/2)\gamma y(\Delta x/y) \\ &\quad \text{for} \quad y/uv_2 < \Delta x < \delta/uv_1 \end{aligned} \quad (36)$$

and vertical $\langle vt\rangle$ and longitudinal $\langle ut\rangle$ heat fluxes can be described with the aid of equation (18):

$$B_{it}(\Delta x/y) \cong \langle it\rangle - \tfrac{9}{16}\Gamma(1/3)Qa_{it}(\Delta x/y)^{4/3} \quad \text{for} \quad \Delta x < y/it_3$$

$$\begin{aligned} B_{it}(\Delta x/y) &\cong \langle it\rangle - Q[0.75a_{it}it_3^{-4/3} \\ &\quad + A_{it}(\gamma + \ln it_2)] - A_{it}Q\ln(\Delta x/y) \\ &\quad \text{for} \quad y/it_2 < \Delta x < H/it_1 \end{aligned} \quad (37)$$

where $\gamma \cong 0.58$ is Euler's constant, $i = u,v$.

5. CONCLUSION

The dimensional theory proves to be very helpful when the turbulent structure of boundary layers with adverse pressure gradient is analyzed. The formulas derived allow us to calculate and compare with experiments such important characteristics of wall flows as spectra and profiles of Reynolds stresses $\langle -uv \rangle$, temperature fluxes $\langle vt \rangle$, $\langle ut \rangle$, second-order moments of turbulent fluctuations of velocity, and temperature in the gradient sublayer of a retarded turbulent flow. Together with the results of theoretical and experimental studies of turbulent structure in a logarithmic sublayer of constant-pressure flows, these results can be used to describe the profile of second-order moments in the most important near wall part of an adverse pressure-gradient boundary layer.

The results above lead to the conclusion that distribution of energy in the low wave number part of the spectra E_u, E_t differs strongly from the spectral distribution in E_v and E_{ut} spectra, but they cannot explain this phenomenon. The contribution of disturbances with low k to the energy of turbulent motions (related to the large-scale organized structures or 'inactive' turbulence which is generated by the large-scale turbulence disturbances in the outer part of the boundary layer) probably affects the vertical and horizontal velocity fluctuations in different ways, but there are no direct experiments to clarify this problem.

All the theoretical formulas deduced above include some unknown constants which can be evaluated from a model using some appropriate closing hypotheses or estimated from the data obtained in experiments. Unfortunately, up until now the necessary experiments have been very rare or absent, so the evaluations of coefficients in the formulas given above must be considered as only preliminary ones and additional experiments are needed to verify the deduced relations, especially those concerning spatial correlation functions.

Acknowledgements—This paper was stimulated by the work in ref. [15] and the author is grateful to Dr A. Yaglom for numerous discussions of the results of this work. The author also thanks Dr I. Marušić, who kindly provided him with his Ph.D. thesis [22], the numerical data of the measured spectra and moments, and a copy of the report in ref. [21].

REFERENCES

1. B. S. Stratford, The prediction of separation of the turbulent boundary layer, *J. Fluid Mech.* **5**, 1–16 (1959); An experimental flow with zero skin friction throughout its region of pressure rise, *J. Fluid Mech.* **5**, 17–35 (1959).
2. A. E. Perry, J. B. Bell and P. N. Joubert, Velocity and temperature profiles in adverse pressure gradient turbulent boundary layers, *J. Fluid Mech.* **25**, 299–320 (1966).
3. P. S. Roganov, Experimental study of heat transfer in a decelerating boundary layer, Candidate Dissertation, Moscow State Technical University, Moscow (1979).
4. B. A. Kader, Heat and mass transfer in pressure-gradient boundary layers, *Int. J. Heat Mass Transfer* **34**, 2837–2857 (1991).
5. B. A. Kader and A. M. Yaglom, Similarity treatment of moving-equilibrium turbulent boundary layers in adverse pressure gradients, *J. Fluid Mech.* **89**, 305–342 (1978).
6. A. S. Ginevskii and E. E. Solodkin, Transverse wall curvature effects on the characteristics of an axially symmetric turbulent boundary layer, *Prikl. Mat. Mech.* (*Appl. Math. Mech.*) **22**, 819–825 (1958).
7. N. Afsal, Thermal boundary layer under strong adverse pressure-gradient near separation, *Trans. ASME, J. Heat Transfer* **104**, 397–402 (1982).
8. P. A. Durbin and S. E. Belcher, Scaling of adverse-pressure-gradient turbulent boundary layers, *J. Fluid Mech.* **238**, 699–722 (1992).
9. K. S. Yajnik, Asymptotic theory of turbulent shear flows, *J. Fluid Mech.* **42**, 411–427 (1970).
10. B. A. Kader, Spectra of anisotropic velocity fluctuations in the gradient sublayer of ecelerating turbulent boundary layers, *Dokl. Akad. Nauk U.S.S.R.* **279**, 323–327 (1984).
11. A. S. Monin and A. M. Yaglom, *Statistical Fluid Mechanics*. Vol. 1. MIT Press, Cambridge, MA (1971).
12. P. A. C. Okwuobi and R. S. Azad, Turbulence in conical diffuser with full developed flow at entry, *J. Fluid Mech.* **57**, 603–622 (1973).
13. R. S. Azad and R. H. Hummel, Similarities of turbulence structure in a conical diffuser with other wall flows, *AIAA J.* **17**, 884–891 (1979).
14. V. M. Belov, Experimental study of heat transfer in turbulent boundary layer at step-changing boundary temperature on a wall, Candidate Dissertation, Moscow State Technical University, Moscow (1976).
15. A. M. Yaglom, Fluctuation spectra and variances in convective turbulent boundary layers: a re-evaluation of old models, *Physics Fluids* **6**, 962–972 (1994).
16. A. M. Yaglom, Laws of small-scale turbulence in atmosphere and ocean, *Izv. Akad. Nauk S.S.S.R., Atmos. Oceanic Phys.* **24**, 919–935 (1981).
17. J. C. Kaimal, J. C. Wyngaard, Y. Izumi and O. R. Coté, Spectral characteristics of surface layer turbulence, *Q. J. R. Meteorol. Soc.* **98**, 563–589 (1972).
18. B. A. Kader and A. M. Yaglom, Spectra and correlation functions of surface-layer atmospheric turbulence in unstable thermal stratification. In *Turbulence and Coherent Structures* (Edited by O. Metais and M. Lesieur), pp. 387–412. Kluwer, Dordrecht (1991).
19. B. A. Kader, Turbulence in "gradient sublayer" of decelerating two-dimensional boundary layers, *Dokl. Akad. Nauk U.S.S.R.* **249**, 298–302 (1979).
20. A. M. Yaglom, Similarity laws for constant pressure and pressure-gradient turbulent wall flows, *A. Rev. Fluid Mech.* **11**, 505–540 (1979).
21. L. F. East, W. G. Sawyer and C. R. Nash, An investigation of the structure of equilibrium turbulent boundary layers, R.A.E Technical Report 79040, London (1979).
22. I. Marušić, The structure of zero and adverse pressure gradient turbulent boundary layers, Ph.D. Thesis, University of Melbourn, Australia (1991).
23. B. A. Kader, A. M. Yaglom and S. L. Zubkovskii, Spatial correlation functions of surface-layer atmospheric turbulence in neutral stratification, *Boundary-Layer Meteorol.* **47**, 233–249 (1989).
24. I. S. Gradshteyn and I. M. Ryzhik, *Tables of Integrals, Sums, Series, and Products*. Academic Press, New York (1980).
25. A. Erdélyi, W. Magnus, F. Oberhettinger and F. G. Tricomi, *Higher Transcendental Functions*, Vol. 2. McGraw-Hill, New York (1953).